Geophysical Research Letters

RESEARCH LETTER
10.1029/2022GL101877

Observed Relationships Between Tropical Cyclone Vortex Height, Intensity, and Intensification Rate

Alexander J. DesRosiers[1], Michael M. Bell[1], Philip J. Klotzbach[1], Michael S. Fischer[2,3], and Paul D. Reasor[3]

[1]Department of Atmospheric Science, Colorado State University, Fort Collins, CO, USA, [2]Cooperative Institute of Marine and Atmospheric Studies, University of Miami, Miami, FL, USA, [3]NOAA AOML Hurricane Research Division, Miami, FL, USA

Key Points:

- Vertical extent of the tropical cyclone wind field correlates strongly with current intensity in observed storms
- Deep vertical vortex structure is always present in observed cases meeting a pressure-based rapid intensification definition
- Vortex height decreases with increasing vertical wind shear, but taller storms intensify more in moderate shear

Supporting Information:

Supporting Information may be found in the online version of this article.

Correspondence to:

A. J. DesRosiers,
adesros@rams.colostate.edu

Citation:

DesRosiers, A. J., Bell, M. M., Klotzbach, P. J., Fischer, M. S., & Reasor, P. D. (2023). Observed relationships between tropical cyclone vortex height, intensity, and intensification rate. *Geophysical Research Letters*, *50*, e2022GL101877. https://doi.org/10.1029/2022GL101877

Received 27 OCT 2022
Accepted 3 MAR 2023

Abstract As a tropical cyclone (TC) intensifies, the tangential wind field expands vertically and increases in magnitude. Observations and modeling support vortex height as an important TC structural characteristic. The Tropical Cyclone Radar Archive of Doppler Analyses with Recentering data set provides kinematic analyses for calculation of the height of the vortex (HOV) in observed storms. Analyses are azimuthally-averaged with tangential wind values taken along the radius of maximum winds. A threshold-based technique is used to determine the HOV. A fixed threshold HOV strongly correlates with current intensity. A dynamic HOV metric quantifies vertical decay of tangential wind with reduced dependency on intensity. Statistically significant differences are present between dynamic HOV values in groups of steady-state, intensifying, and rapidly-intensifying cases categorized by subsequent changes in pressure. A tall vortex is always observed in cases meeting a pressure-based rapid intensification definition. Taller vortices are also evident with slower intensification. Results suggest HOV may be a helpful predictor for TC intensification.

Plain Language Summary As a tropical cyclone gets stronger, the wind field of the storm grows taller in the atmosphere. The height-intensity relationship is known to be present from the beginning of a tropical cyclone until its peak strength. A large data set of airborne radar observations in tropical cyclones is used to show the strength of the relationship between vortex height and current intensity. A tall vortex is always present in observed cases for periods of rapid intensification during which the minimum surface pressure at the storm center drops at a high rate. Drops in minimum surface pressure are associated with increases in wind and size in tropical cyclones. A taller vortex also favors intensification at slower rates. Improved understanding of the role that tropical cyclone height plays during intensification may be helpful for forecasting changes in intensity of these storms.

1. Introduction

Tropical cyclones (TCs) have long been understood as a phenomena capable of spanning a large depth of the troposphere (Haurwitz, 1935). While TCs are known to exhibit deep convection throughout their life cycle, the evolution of the vertical structure of the wind field is still not fully understood. Tangential wind profiles in TCs obtained during reconnaissance in the 1950s and 1960s showed early evidence of a link between increased upper-level inner-core tangential wind and TC intensification rate (Fitzpatrick, 1995). Evidence suggests that even during the pre-genesis stage of the TC life cycle, the height of the circulation is important. A deep wave pouch in which a TC forms is likely a necessary condition for genesis from an easterly wave (Wang et al., 2012). Once a TC has formed, idealized numerical simulations indicate a deeper initial vortex may undergo faster intensification (Peng & Fang, 2021). In a mature TC, vortical flow can continue to reach higher altitudes. Tail Doppler radar (TDR) data collected in Hurricane Patricia (2015) near peak intensity documented an intense axisymmetric vortex with strong tangential winds extending vertically through the depth of the troposphere (Martinez et al., 2019; Rogers et al., 2017).

As a TC becomes more intense, upper-level dynamics and thermodynamics take on greater importance while the vortex grows vertically. Inertial stability decays quickly with height in shallower vortices, likely impacting heating efficiency in the inner-core (Schubert & Hack, 1982). Composite observations indicate updraft mass flux peaks at higher altitudes and decreases less rapidly with height in intensifying storms (Rogers et al., 2013). Rapid intensification (RI) is canonically defined as an increase in the maximum sustained winds

of a TC of at least 30 kts in a 24-hr period (Kaplan & DeMaria, 2003; Kaplan et al., 2010). Successful prediction of RI is difficult (Trabing & Bell, 2020), due in part to the importance of internal dynamical processes in otherwise favorable environments for intensification (Hendricks et al., 2010). DesRosiers et al. (2022) analyzed TDR data from Hurricane Michael (2018) to show how the axisymmetric eyewall vorticity tower grew vertically during RI which occurred during the majority of its lifetime. They argued thermal wind balance linked the upper-level warm core development with changes in vertical structure of the tangential wind field during RI.

Other aspects of TC vertical structure have received attention in observational analysis. Hazelton and Hart (2013) examined the vertical slope of eyewalls in Atlantic hurricanes and documented a greater slope at upper levels than at lower levels. Stern and Nolan (2009) evaluated vertical structure of the radius of maximum winds (RMW). Their observations showed the RMW is approximately a surface of constant absolute angular momentum, and outward slope of the RMW increases with RMW size. Follow-on work investigated the profile of tangential wind field decay with height scaled by the lower-level wind maximum. Although theoretical arguments suggest uniformity in the decay profile, observational data indicate a tendency for the decay to decrease with increasing TC intensity and decreasing TC size (Stern & Nolan, 2011; Stern et al., 2014). Collections of aircraft reconnaissance data offer an excellent opportunity to make discoveries about TC structure relative to intensity change (Martinez et al., 2017; Rogers et al., 2013). While prior research suggests that important relationships between height of the TC vortex, TC intensity, and TC intensification rate exist, these relationships have not been fully explored. In this study, aircraft radar observations from multiple TCs are used to characterize the relationships between vortex height and current intensity as well as intensification.

2. Data and Methods

NOAA P-3 Hurricane Hunter aircraft reconnaissance research flights equipped with a TDR collect data to document TC inner-core structure. The Tropical Cyclone Radar Archive of Doppler Analyses with Recentering (TC-RADAR) is a large observational data set of inner-core kinematic analyses derived from TDR data (Fischer et al., 2022). TC-RADAR is used herein to investigate how TC vertical structure relates to intensity and intensification. The version of TC-RADAR (v3j) used contains 306 merged analyses assembled using all TDR data collected during a flight. Data are typically collected in a series of radial aircraft legs crossing the TC center. TC-RADAR analyses are in Cartesian coordinates with a horizontal and vertical resolution of 2 and 0.5 km, respectively, with a vertical domain extending from the surface to 18 km. Cases in TC-RADAR where the storm was within 50 km of land were excluded to limit impacts of surface heterogeneity on inner-core structure. The 50 km threshold does not entirely eliminate surface heterogeneity impacts, but is consistent with the exclusion criterion used by Fischer et al. (2022). Cases where the TC minimum sea level pressure was greater than 1,000 hPa were excluded as they often do not have a coherent azimuthally-averaged vertical structure to analyze. If two flights were close enough together to share a 6-hourly synoptic time and duplicate intensity and intensity change information, only the flight closest to the 6-hourly synoptic time was retained. Two hundred twenty-three cases remained after exclusion criteria were applied. The majority of cases are in the North Atlantic with ∼3% from the eastern North Pacific.

The process to obtain the height of the TC vortex (HOV) is illustrated using an analysis of Hurricane Florence (2018) (Figure 1). The tangential wind field for a merged analysis of interest (Figure 1a) is converted from Cartesian to cylindrical coordinates with a resolution of 0.5 km, 2.0 km, and 1° in the vertical, radial, and azimuthal dimensions, respectively. The cylindrical field is azimuthally averaged (Figure 1b). A 25% data coverage filter is applied when averaging the cylindrical field in the azimuthal dimension to prevent isolated data points from being unrepresentative of the averaged field in radius-height space. The RMW (cyan; Figure 1b) is calculated from the full wind field composed of radial and tangential components by identifying the radius at which the greatest wind is observed at each vertical level. Tangential wind speed at the RMW is recorded at all vertical levels. Several potential threshold values, which are evaluated in the next section, are used to determine useful HOV definitions. The greatest height at which the maximum value exceeds or is equal to the threshold value is the HOV. If the value is never exceeded or equaled, the HOV is considered to be 0 km. The threshold technique is also applicable for other dynamical fields available in TC-RADAR, but this study focuses on tangential wind. Two HOV values (HOV24 and dynamic HOV) obtained using the described method are noted in the example case (Figure 1b). Their definitions and importance to TC intensity and intensity change are provided in the following section.

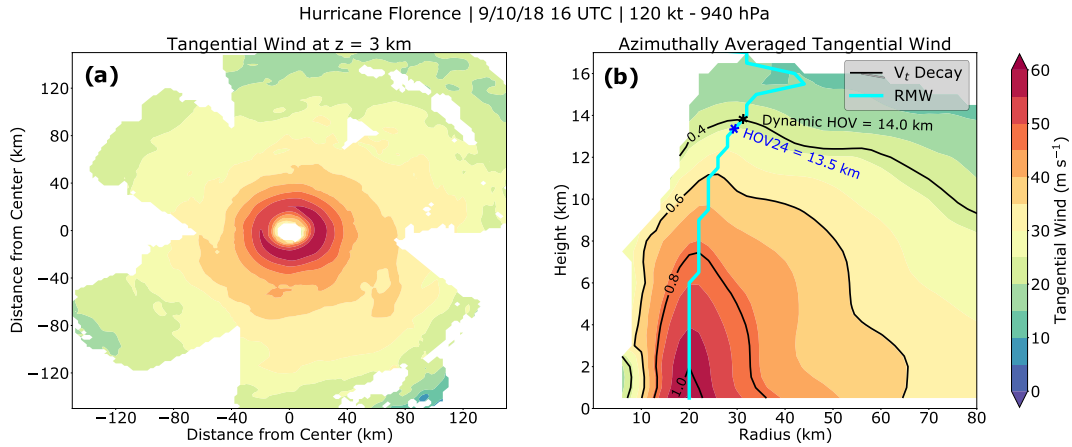

Figure 1. (a) Merged tangential wind analysis at a height (z) of 3 km from TC-RADAR in Hurricane Florence at Category 4 intensity and (b) the azimuthally-averaged tangential wind field. The radius of maximum winds (RMW) is denoted by a cyan contour. Black contours are tangential wind (V_t) divided by the maximum value of V_t found at the RMW at z of 2 km.

3. Results

The previously-described methodology is used to compute and analyze HOV metrics. An example case is highlighted where HOV could have provided helpful diagnostic information for predicting intensity change.

3.1. Vortex Height and Intensity

The tangential wind field was used with the threshold method to define a vortex height metric that correlates well with the current intensity of observed TCs in TC-RADAR. Tangential wind thresholds ranging from 16 to 28 m s^{-1} were used to determine the HOV in Figure 2. With a lower threshold, many cases failed to capture the threshold value along the RMW within the vertical domain of resolved azimuthally-averaged winds of the TDR analysis (Figure 2b). Conversely, higher threshold values failed in cases with tangential winds that did not exceed this value (Figure 2a), resulting in an HOV of 0 km. Correlations of HOV values at each threshold with intensity as defined by V_{max}, or the maximum sustained 10 m winds (Figure 2c), and P_{min}, or minimum sea level pressure (Figure 2d), were calculated and tracked. The percentage of cases without an explicitly observed HOV and correlations with intensity at each threshold were used to subjectively determine an optimal threshold value. HOV as determined by the 24 m s^{-1} tangential wind threshold (gray - dashed; Figures 2a–2d), or HOV24, exists at a point where the slope of mutual increases in correlation with threshold lessens, and cases with no observed HOV remain low, representing a reasonable compromise between constraints.

HOV24 was directly observed in ∼71% of the 223 cases analyzed. HOV24 showed a strong linear relationship with present storm intensity as defined by V_{max} (Figure 2e) and P_{min} (Figure 2f) with linear correlation values of ∼0.9 for both. Spearman's rank correlations are slightly stronger with values of ∼0.92 and 0.93 for V_{max} and P_{min}, respectively. Some non-linearity in the scatter can be explained at the low end where observed azimuthally-averaged tangential winds are weaker than 24 m s^{-1} in some cases. At higher altitudes, asymptotic behavior is likely due in part to TDR sensitivity limitations. Color coding of the dots in the scatter (Figures 2e and 2f) indicate categorical classifications of intensity change determined by temporal changes in P_{min} (legend; Figure 2e) described in the following subsection. Quantification of the known mutually-increasing relationship between vertical depth and intensity in TCs (Fischer et al., 2022; Stern et al., 2014) in a novel observational data set exhibits the potential utility of this methodology to explore connections between vortex height and intensity change.

3.2. Relationship With Intensity Change

A key argument to the importance of the vertical development observed during the RI of Hurricane Michael (DesRosiers et al., 2022) was the integral nature of P_{min} as an intensity metric. As the vortex grew in height, geopotential height decreases aloft helped contribute to a reduction of P_{min} at the surface. Given the hydrostatic

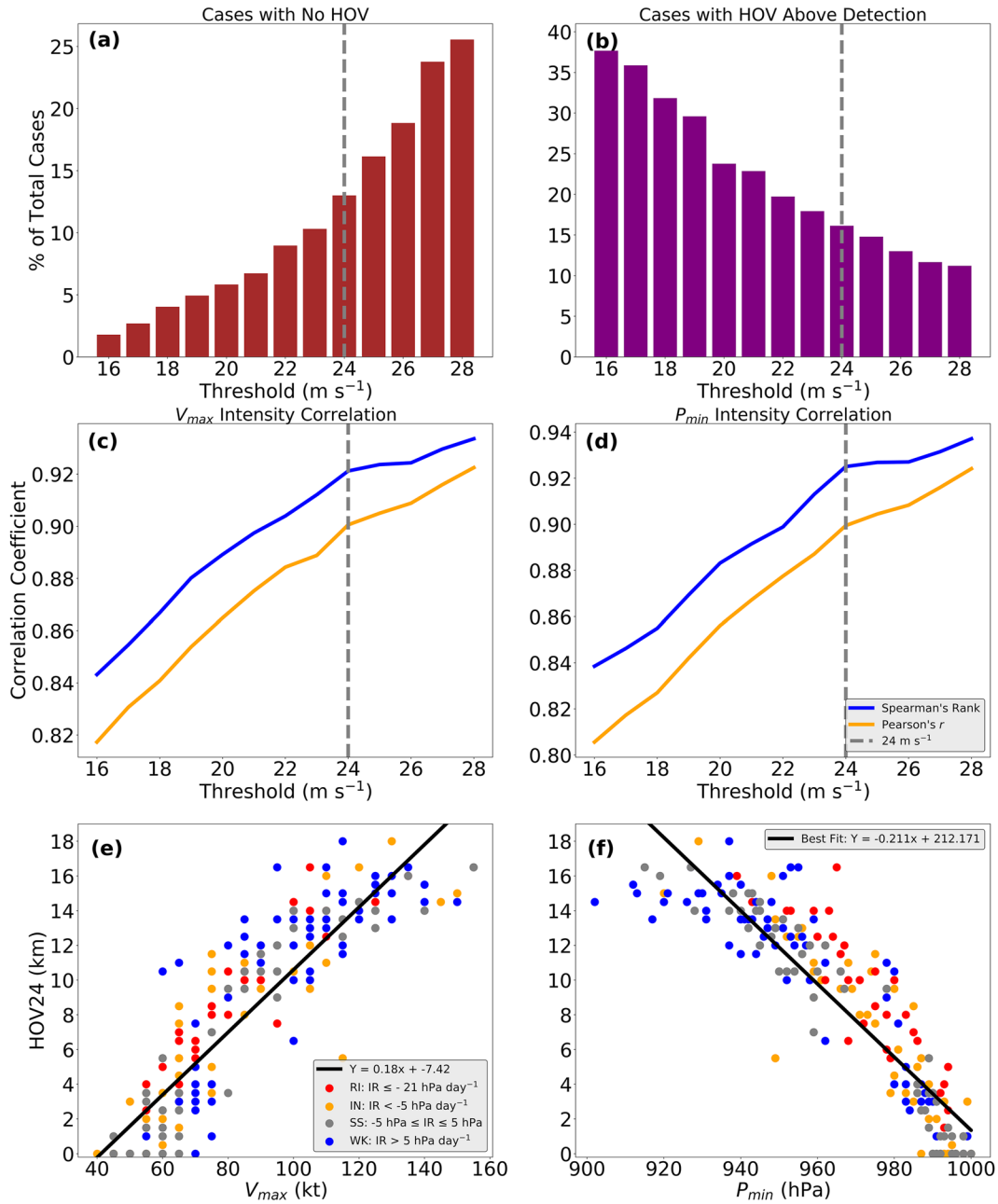

Figure 2. Percentage of all cases ($n = 223$) at each tangential wind threshold where HOV is (a) not recorded or (b) occurs above detection range. Spearman's rank (blue) and Pearson's r (orange) correlation coefficients of HOV with current intensity defined by (c) V_{max} and (d) P_{min}. HOV defined by the 24 m s^{-1} contour (HOV24) for all cases plotted against intensity as defined by (e) V_{max} and (f) P_{min}. Observations are grouped and labeled by intensification rate (IR) following analysis time (colors - legend).

link between vortex height and surface P_{min}, the relationship between HOV and intensity change is examined through changes in pressure, where the relationship is stronger than the one obtained using wind. Structural factors which can lower P_{min} are important to understand as P_{min} correlates better with normalized damage in continental US landfalling hurricanes than V_{max} (Klotzbach et al., 2020, 2022). We hypothesize that geopotential height falls aloft in a deeper vortex are associated with a more efficient reduction of P_{min}, which is an integrated metric of the three-dimensional wind field through thermal wind balance.

Cases from TC-RADAR are divided into four intensity change categories based on the 24-hr change in P_{min} following storm analysis time given in TC-RADAR. Aircraft reconnaissance missions are most common in TCs

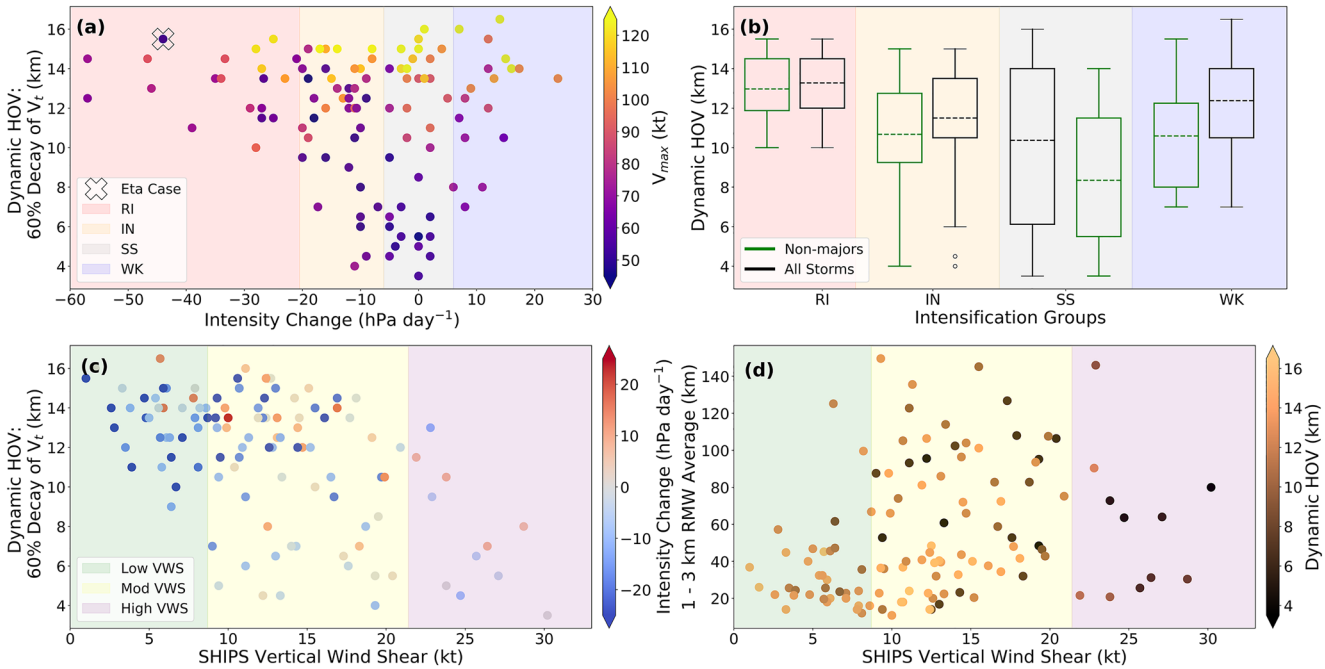

Figure 3. (a) Dynamic HOV determined by 60% decay of tangential wind with respect to its value at height (z) of 2 km as a function of intensity change. Intensity of storm at analysis time (colorbar) as well as intensity change groups (shaded) are shown. Two WK cases occupy the x,y coordinate pairs of (8,7), (9,13), and (12,15.5) with the intensities of each case pair within 5 kt of each other. A hollow X surrounds the Hurricane Eta (2020) case discussed in Section 3. (b) Box and whisker plots with means (dashed) for each intensity change grouping for all storms (black) and non-major hurricane strength storms (green). (c) Differences in dynamic HOV for different regimes of vertical wind shear with low, moderate, and high values shaded. 24-hour change in pressure following the analysis time (colorbar) is shown for each point. (d) Dynamic HOV values (colorbar) in cases with varying shear and low-level (z = 1–3 km) averaged RMW.

threatening land. Restricting to only cases where a full 24-hr period occurred over water further limits the sample size due to the many landfalling TCs observed. If landfall occurred in the final 6 hr (11 of 116 cases in the final data set), the analysis was retained in addition to purely over water cases, and the 18-hr over water intensification rate was extrapolated to 24 hr assuming a constant rate. The RI category boundary is determined with a method consistent with its original calculation with respect to V_{max} (Kaplan & DeMaria, 2003). The equivalent 95th percentile of over water intensity change for pressure-based RI is a 21 hPa drop in P_{min} in 24 hr, when considering the period of 1979–2021 for the North Atlantic (Landsea & Franklin, 2013). Cases with pressure drops greater than 5 hPa, but not crossing the RI threshold make up the intensifying (IN) group. Changes in P_{min} from −5 to +5 hPa are considered steady-state (SS). Increases in pressure greater than 5 hPa are classified as weakening (WK).

Metrics using specific thresholds like HOV24 have strong correlations with present intensity, so a value reflective of vortex height with decreased sensitivity to present intensity is introduced as dynamic HOV. Dynamic HOV is obtained with the same thresholding approach along the RMW, however, the threshold is now specific to the intensity of each case. The threshold is 40% of the value of the maximum tangential wind at 2 km altitude (Figure 1b) due to its greater relationship with intensity change compared to other thresholds investigated (not shown). Scaling decay with the 2-km maximum tangential wind is consistent with previous work investigating wind field decay (Stern et al., 2014; Stern & Nolan, 2011). The HOV is set as the last vertical level where this threshold is equaled or exceeded along the RMW as defined by the full wind field. For inclusion of a case in dynamic HOV analysis, the threshold value must be explicitly observed. One hundred sixteen cases were qualified for analysis with counts of 20, 41, 34, and 21 in the RI, IN, SS, and WK groups, respectively. Of the 223 original cases, dynamic HOV was not observed in 77, and 30 did not have at least 18 hr over water after analysis.

Plotting dynamic HOV values against intensity change (Figure 3a) reveals a narrowing of the range of values toward higher HOV as the intensification rate becomes greater. The present intensity of TC cases (colors; Figure 3a) shows some relationship with dynamic HOV, consistent with previously-calculated profiles of observed vertical wind field decay (Fischer et al., 2022; Stern et al., 2014). Storms of major (Category 3+; ≥96 kt) intensity on the

All Storms

(a)	RI	IN	SS	WK
RI		0.03	0.03	0.47*
IN	0.03		0.43	0.22*
SS	0.03	0.43		0.1
WK	0.47*	0.22*	0.1	

Non-Majors

(b)	RI	IN	SS	WK
RI		<0.01	<0.01	0.03
IN	<0.01		0.02	0.77
SS	<0.01	0.02		0.06
WK	0.03	0.77	0.06	

Figure 4. Two-sided p-values for Mann-Whitney U tests between intensification groups for (a) all storms and (b) excluding major hurricanes. White squares indicate a failure to reject the null hypothesis, while green squares are statistically significant differences at the 95% confidence level. Results with an asterisk indicate statistically significant differences in present intensity between groups.

Saffir-Simpson Hurricane Wind Scale typically have a deep vertical structure indicated by high dynamic HOV values which vary little. Non-major cases possess considerable variability. Box and whisker plots with dashed mean values (Figure 3b) show a tendency of increasing dynamic HOV as the intensification rate moves toward RI. The increasing trend is most prevalent in non-major cases (green) which is consistent with the increased upper-level tangential winds found in intensifying storms of tropical storm to lower-end hurricane intensity (Fitzpatrick, 1995). In general, the results suggest a tall vortex may be a necessary condition for pressure-based RI in the observed data set. The result relates well with findings of a comparison study (Hazelton et al., 2018) in which modeled Atlantic TCs exhibited higher than observed intensities and a greater vortex depth parameter based on V_t decay when compared to TDR observations.

The relationship between dynamic HOV and intensity change must also be considered in the context of vertical wind shear (VWS). Vortex height is determined through azimuthal averaging about a lower-tropospheric center, so a tilting of the vortex by VWS (Jones, 1995) can stunt the height of the vortex when it is unable to be aligned upright about its center, weakening the azimuthally-averaged projection of tangential winds. SHIPS VWS (SHDC: deep-layer shear with vortex removed) magnitude at analysis time (DeMaria et al., 2005) is examined in three different categories of low, moderate, and high as defined in Rios-Berrios and Torn (2017), a climatological study focused on the challenges of TC intensity change prediction in moderate VWS. Moderate VWS falls between and including the magnitudes of 8.7 and 21.4 kt with low and high ranges on the opposite ends of these bounds, respectively. Dynamic HOV tends to be higher in low VWS environments and lower in high VWS environments. There is substantial variability in the moderate VWS regime (Figure 3c). Cases with a greater reduction in $P_{\min}$ occurring in moderate shear tend to have higher dynamic HOV. The radial extent of the circulation also appears to be related to the dynamic HOV. TCs with more compact inner cores, as evidenced by the $z = 1$–3 km RMW average value, are more likely to have higher dynamic HOV values (Figure 3d). Low VWS environments also tend to favor a more compact inner-core, which is known to be conducive to RI (Carrasco et al., 2014).

Significance testing is used to determine if there are statistically significant differences between dynamic HOV values in intensity change groups for all storms and non-major cases. The Mann-Whitney U two-tailed non-parametric test (Nachar, 2008) is chosen to determine if the null hypothesis can be rejected, and the distributions of dynamic HOV values between two groups can be considered different from each other. Results of the statistical tests are given as matrices in Figure 4 where two-sided p-values in highlighted green boxes denote rejection of the null hypothesis at the 95% confidence level. Distributions of dynamic HOV values for RI were found to be different from IN and SS groups in both categories. Differences between the IN and SS groups were also statistically significant for non-majors, but confidence in this particular result drops to 94% when a tangential-wind-defined RMW is used. Lower p-values for non-majors indicates the relationship between greater dynamic HOV and RI is driven by weaker cases. The majority of observed wind-based RI cases in the Atlantic initiate below hurricane strength (Kaplan & DeMaria, 2003). The same two-tailed Mann-Whitney U test was used to probe for differences in the current intensity via $P_{\min}$ in the groups (Figure 3a). An asterisk (Figure 4) indicates a comparison between groups where the null hypothesis that the present intensity distribution was the same could be rejected, and differences in intensity may impact differences in dynamic HOV. Of the statistically significant differences found in dynamic HOV, none were flagged for intensity differences. Although not marked as significant, the mean $P_{\min}$ of the RI group is ∼2 hPa less than the IN group for all storms and ∼6 hPa for

non-majors. Some differences in intensity between RI and IN are expected given previous research showing that as a TC grows more intense, the heating efficiency increases as well (Nolan et al., 2007; Schubert & Hack, 1982), likely enabling greater pressure falls. Mean dynamic HOV values of the WK cases were not less than SS, but this may be due to mean intensity differences. Some WK storms of lesser intensity were also previously major hurricanes with established tall vortices. The average peak lifetime intensity of the WK cases is ∼115 kt. The timescale of decay of the vertical structure in weakening TCs and what controls the decay rate is a topic for future investigation.

Example Case: Hurricane Eta Dynamic HOV may have been an early indicator in the extreme RI event preceding major Hurricane Eta's (2020) landfall in Nicaragua. A flight centered around 19 UTC on 1 November 2020 sampled Eta as a 50 kt tropical storm with P_{min} of 992 hPa in a favorable environment. The National Hurricane Center forecast Eta to intensify in their 21 UTC advisory issued later that day. The forecast called for a strengthening 80 kt Category 1 hurricane at 18 UTC on 2 November 2020. Eta far exceeded expectations and became a 115 kt Category 4 hurricane with P_{min} of 948 hPa by the verification time (Pasch et al., 2021). Dynamic HOV calculated from the 1 November flight into then Tropical Storm Eta was an impressive 15.5 km (Figure 3a), indicating a vertical structure that we hypothesize was conducive for its subsequent RI event (Figure S1).

4. Conclusions

Previous studies have shown that the height of the tropical cyclone (TC) vortex (HOV) is an important structural factor in the TC life cycle. A comprehensive data set of TDR-derived kinematic observations of TCs makes possible the characterization of relationships between vortex height and TC intensity and intensification. A threshold-focused technique is used to determine the HOV based on tangential wind values along the radius of maximum winds (RMW). HOV as determined by the 24 m s^{-1} (HOV24) tangential wind threshold offered the best compromise between number of cases where the value is directly observed and correlations with present intensity. Correlation values are ∼0.9 for HOV24 and intensity as defined by wind and pressure. These results provide strong and novel observational evidence of the known relationship between vortex height and TC intensity (Fischer et al., 2022; Stern et al., 2014).

Rapid intensification (RI) in TCs is challenging to predict and controlled by internal dynamical processes in addition to environmental factors. A more general understanding of the role vertical structure plays should improve understanding of internal mechanisms during RI. RI is defined in this study in a similar manner to the original, wind-based definition using rates of decrease in P_{min} which yielded a stronger signal than rates of increase in V_{max}. Each case in the data set is grouped into rapidly intensifying (RI), intensifying (IN), steady-state (SS), and weakening (WK) groups based on a 24-hr change in P_{min} following analysis time. Dynamic HOV, which is determined by the height at which the tangential wind along the RMW decays to 40% of its value at a height of 2 km, is used due to its lower sensitivity to present intensity as compared to a fixed threshold. As decreases in pressure following the analysis time become greater, the distribution of dynamic HOV values narrows and becomes composed of exclusively higher values. The mean dynamic HOV increases from SS toward RI groups for all storms. The increase in mean dynamic HOV is greater when only considering cases below major hurricane intensity, at which point a deep vortex is expected in a major storm. Lower vertical wind shear (VWS) values and smaller inner-core size favor greater dynamic HOV values. Higher dynamic HOV favors intensification in moderate VWS. The VWS relationship may indicate that larger HOV values are associated with more aligned vortices, but a more thorough analysis is needed. We hypothesize that a deeper vortex can more efficiently lower P_{min} and intensify in high dynamic HOV cases. How and if this puzzle piece fits uniquely into the TC intensification process, or is a symptom of other mechanisms, needs further investigation.

Significant differences exist between the distribution of dynamic HOV values in RI groups when compared to IN and SS prior to the change in intensity. Differences between the IN and SS groups were also found to be statistically significant in cases when excluding major hurricanes. The statistical significance of the dynamic HOV and intensification relationship is mainly defined by cases of lower intensity which possess more variability in dynamic HOV. Dynamic HOV may be useful for predicting TC intensity change in relatively weak TCs. WK cases had mean dynamical HOV values in excess of SS cases, which may be due in part to the small sample size, stronger mean current intensity, and some of the weaker cases being major hurricanes previously. The timescale of both the growth and decay of vertical structure in a TC should be investigated in future studies. The age of the TC and its potential relationship with dynamic HOV should also be investigated. The recent example case

of Eta (2020) and its extreme RI event illustrates that dynamic HOV might be useful in forecasting TC intensity change. Future work should focus on both achieving a greater understanding of the mechanisms involved with vortex height and intensity change as well as identifying ways to utilize height-based metrics for real-time TC intensity forecasting.

Data Availability Statement

HOV metrics calculated in TC-RADAR are available on Figshare at http://doi.org/10.6084/m9.figshare.21375804. TC-RADAR (version v3j) can be accessed at www.aoml.noaa.gov/ftp/pub/hrd/data/radar/level3/.

Acknowledgments
This research is supported by ONR award N000142012069. The authors thank Patrick Fitzpatrick for prior motivating work. The authors thank Andrew Hazelton and an anonymous reviewer for helpful comments and suggestions.

References

Carrasco, C. A., Landsea, C. W., & Lin, Y.-L. (2014). The influence of tropical cyclone size on its intensification. *Weather and Forecasting*, *29*(3), 582–590. https://doi.org/10.1175/WAF-D-13-00092.1

DeMaria, M., Mainelli, M., Shay, L. K., & Knaff, J., John, A., & Kaplan. (2005). Further improvements to the Statistical Hurricane Intensity Prediction Scheme (SHIPS). *Weather and Forecasting*, *20*(4), 531–543. https://doi.org/10.1175/WAF862.1

DesRosiers, A. J., Bell, M. M., & Cha, T.-Y. (2022). Vertical vortex development in Hurricane Michael (2018) during rapid intensification. *Monthly Weather Review*, *150*(1), 99–114. https://doi.org/10.1175/MWR-D-21-0098.1

Fischer, M. S., Reasor, P. D., Rogers, R. F., & Gamache, J. F. (2022). An analysis of tropical cyclone vortex and convective characteristics in relation to storm intensity using a novel airborne Doppler radar database. *Monthly Weather Review*, *150*(9), 2255–2278. https://doi.org/10.1175/MWR-D-21-0223.1

Fitzpatrick, P. J. (1995). *Understanding and forecasting tropical cyclone intensity change* (Unpublished doctoral dissertation). Colorado State University.

Haurwitz, B. (1935). The height of tropical cyclones and the "eye" of the storm. *Monthly Weather Review*, *63*(2), 45–49. https://doi.org/10.1175/1520-0493(1935)63<45:thotca>2.0.co;2

Hazelton, A. T., Harris, L., & Lin, S.-J. (2018). Evaluation of tropical cyclone structure forecasts in a high-resolution version of the Multiscale GFDL fvGFS Model. *Weather and Forecasting*, *33*(2), 419–442. https://doi.org/10.1175/WAF-D-17-0140.1

Hazelton, A. T., & Hart, R. E. (2013). Hurricane eyewall slope as determined from airborne radar reflectivity data: Composites and case studies. *Weather and Forecasting*, *28*(2), 368–386. https://doi.org/10.1175/WAF-D-12-00037.1

Hendricks, E. A., Peng, M. S., Fu, B., & Li, T. (2010). Quantifying environmental control on tropical cyclone intensity change. *Monthly Weather Review*, *138*(8), 3243–3271. https://doi.org/10.1175/2010MWR3185.1

Jones, S. C. (1995). The evolution of vortices in vertical shear. I: Initially barotropic vortices. *Quarterly Journal of the Royal Meteorological Society*, *121*(524), 821–851. https://doi.org/10.1002/qj.49712152406

Kaplan, J., & DeMaria, M. (2003). Large-scale characteristics of rapidly intensifying tropical cyclones in the North Atlantic basin. *Weather and Forecasting*, *18*(6), 1093–1108. https://doi.org/10.1175/1520-0434(2003)018⟨1093:LCORIT⟩2.0.CO;2

Kaplan, J., DeMaria, M., & Knaff, J. A. (2010). A revised tropical cyclone rapid intensification index for the Atlantic and Eastern North Pacific basins. *Weather and Forecasting*, *25*(1), 220–241. https://doi.org/10.1175/2009WAF2222280.1

Klotzbach, P. J., Bell, M. M., Bowen, S. G., Gibney, E. J., Knapp, K. R., & Schreck, C. J., III. (2020). Surface pressure a more skillful predictor of normalized hurricane damage than maximum sustained wind. *Bulletin of the American Meteorological Society*, *101*(6), E830–E846. https://doi.org/10.1175/BAMS-D-19-0062.1

Klotzbach, P. J., Chavas, D. R., Bell, M. M., Bowen, S. G., Gibney, E. J., & Schreck, C. J., III. (2022). Characterizing continental us hurricane risk: Which intensity metric is best? *Journal of Geophysical Research: Atmospheres*, *127*(18), e2022JD037030. https://doi.org/10.1029/2022JD037030

Landsea, C. W., & Franklin, J. L. (2013). Atlantic hurricane database uncertainty and presentation of a new database format. *Monthly Weather Review*, *141*(10), 3576–3592. https://doi.org/10.1175/MWR-D-12-00254.1

Martinez, J., Bell, M. M., Rogers, R., & Doyle, J. D. (2019). Axisymmetric potential vorticity evolution of Hurricane Patricia (2015). *Journal of the Atmospheric Sciences*, *76*(7), 2043–2063. https://doi.org/10.1175/JAS-D-18-0373.1

Martinez, J., Bell, M. M., Vigh, J. L., & Rogers, R. F. (2017). Examining tropical cyclone structure and intensification with the flight+ dataset from 1999 to 2012. *Monthly Weather Review*, *145*(11), 4401–4421. https://doi.org/10.1175/MWR-D-17-0011.1

Nachar, N. (2008). The Mann-Whitney U: A test for assessing whether two independent samples come from the same distribution. *Tutorials in Quantitative Methods for Psychology*, *4*(1), 13–20. https://doi.org/10.20982/tqmp.04.1.p013

Nolan, D. S., Moon, Y., & Stern, D. P. (2007). Tropical cyclone intensification from asymmetric convection: Energetics and efficiency. *Journal of the Atmospheric Sciences*, *64*(10), 3377–3405. https://doi.org/10.1175/JAS3988.1

Pasch, R. J., Reinhart, B. J., & Berg, R. (2021). National Hurricane Center tropical cyclone report: Hurricane Eta (AL292020) NHC Tech. Rep.

Peng, K., & Fang, J. (2021). Effect of the initial vortex vertical structure on early development of an axisymmetric tropical cyclone. *Journal of Geophysical Research: Atmospheres*, *126*(4), e2020JD033697. https://doi.org/10.1029/2020JD033697

Rios-Berrios, R., & Torn, R. D. (2017). Climatological analysis of tropical cyclone intensity changes under moderate vertical wind shear. *Monthly Weather Review*, *145*(5), 1717–1738. https://doi.org/10.1175/MWR-D-16-0350.1

Rogers, R. F., Aberson, S., Bell, M. M., Cecil, D. J., Doyle, J. D., Kimberlain, T. B., et al. (2017). Rewriting the tropical record books: The extraordinary intensification of Hurricane Patricia (2015). *Bulletin of the American Meteorological Society*, *98*(10), 2091–2112. https://doi.org/10.1175/BAMS-D-16-0039.1

Rogers, R. F., Reasor, P., & Lorsolo, S. (2013). Airborne Doppler observations of the inner-core structural differences between intensifying and steady-state tropical cyclones. *Monthly Weather Review*, *141*(9), 2970–2991. https://doi.org/10.1175/MWR-D-12-00357.1

Schubert, W. H., & Hack, J. J. (1982). Inertial stability and tropical cyclone development. *Journal of the Atmospheric Sciences*, *39*(8), 1687–1697. https://doi.org/10.1175/1520-0469(1982)039⟨1687:ISATCD⟩2.0.CO;2

Stern, D. P., Brisbois, J. R., & Nolan, D. S. (2014). An expanded dataset of hurricane eyewall sizes and slopes. *Journal of the Atmospheric Sciences*, *71*(7), 2747–2762. https://doi.org/10.1175/JAS-D-13-0302.1

Stern, D. P., & Nolan, D. S. (2009). Reexamining the vertical structure of tangential winds in tropical cyclones: Observations and theory. *Journal of the Atmospheric Sciences*, *66*(12), 3579–3600. https://doi.org/10.1175/2009JAS2916.1

Stern, D. P., & Nolan, D. S. (2011). On the vertical decay rate of the maximum tangential winds in tropical cyclones. *Journal of the Atmospheric Sciences*, *68*(9), 2073–2094. https://doi.org/10.1175/2011JAS3682.1

Trabing, B. C., & Bell, M. M. (2020). Understanding error distributions of hurricane intensity forecasts during rapid intensity changes. *Weather and Forecasting*, *35*(6), 2219–2234. https://doi.org/10.1175/WAF-D-19-0253.1

Wang, Z., Montgomery, M. T., & Fritz, C. (2012). A first look at the structure of the wave pouch during the 2009 PREDICT-GRIP dry runs over the Atlantic. *Monthly Weather Review*, *140*(4), 1144–1163. https://doi.org/10.1175/MWR-D-10-05063.1